

Diagnosing COVID-19 From Chest CT Scan Images Using Deep Learning Models

Shamik Tiwari, University of Petroleum and Energy Studies, India

 <https://orcid.org/0000-0002-5987-7101>

Anurag Jain, University of Petroleum and Energy Studies, India*

 <https://orcid.org/0000-0001-5155-022X>

Sunil Kumar Chawla, University Institute of Engineering, Chandigarh University, India

 <https://orcid.org/0000-0001-5316-3039>

ABSTRACT

A novel coronavirus named COVID-19 has spread speedily and has triggered a worldwide outbreak of respiratory illness. Early diagnosis is always crucial for pandemic control. Compared to RT-PCR, chest computed tomography (CT) imaging is the more consistent, concrete, and prompt method to identify COVID-19 patients. For clinical diagnostics, the information received from computed tomography scans is critical. So there is a need to develop an image analysis technique for detecting viral epidemics from computed tomography scan pictures. Using DenseNet, ResNet, CapsNet, and 3D-ConvNet, four deep machine learning-based architectures have been proposed for COVID-19 diagnosis from chest computed tomography scans. From the experimental results, it is found that all the architectures are providing effective accuracy, of which the COVID-DNet model has reached the highest accuracy of 99%. Proposed architectures are accessible at <https://github.com/shamiktiwari/CTscanCovi19> and can be utilized to support radiologists and reserachers in validating their initial screening.

KEYWORDS

3-D ConvNet, CapsNet, Chest CT-Scan, COVID-19, Deep Machine Learning, DenseNet, ResNet

INTRODUCTION

A global pandemic has been resulting from the *COVID – 19* virus, which was detected in November 2019. This virus shares genetic similarities with the SARS virus, which was discovered in 2002. This virus was created in bats and then transmitted to humans through them (Jahangir et al., 2020). This virus can spread via the air through water droplets released by affected people while sneezing, speaking, or coughing, and can be active for up to three hours (Alpaydin et al., 2021). The virus is also capable of surviving on the surfaces of objects for a very long time (Bhardwaj et al., 2021).

DOI: 10.4018/IJRQEH.299961

*Corresponding Author

This article published as an Open Access article distributed under the terms of the Creative Commons Attribution License (<http://creativecommons.org/licenses/by/4.0/>) which permits unrestricted use, distribution, and production in any medium, provided the author of the original work and original publication source are properly credited.

COVID – 19 is more common in people over 60, children under the age of 12, asthmatic patients, people with weakened immune systems, and pregnant women. The earliest signs of *COVID – 19* are a high temperature, exhaustion, low breath, cough, loss of aroma and flavor. Later on, this progresses to serious lung damage, which is referred to as acute respiratory distress syndrome in medical terms (ARDS). After five days of infection, a person develops *COVID – 19* symptoms. The incubation period is five days, and during this time, a *COVID – 19* affected individual becomes a moving source of infection (Jain et al., 2021). At the moment, one individual affected with *COVID – 19* is infecting another 2.2 people. A doctor can utilize the RT-PCR test to confirm the condition. This method can also identify a trace amount of viral ribonucleic acid (RNA). At the initial stage, however, this test fails to identify the *COVID – 19* virus (Tahamtan & Ardebili, 2020). A clinician can diagnose lung disease resulting from *COVID – 19* infection utilizing chest CT (Computed Tomography) scans. Other approaches for detecting *COVID – 19* include serological testing. This approach looks for antibodies produced by the immune system to attack the virus to determine the presence of the *COVID – 19* virus (Lee et al., 2020). The sensitivity of the RT-PCR test was between 30 and 70% at the start of the pandemic. The sensitivity of the second generation RT-PCR test has increased to 95%, making it more accurate than a chest x-ray. However, the RT-PCR test still has issues with waiting times, test costs, and the lack of testing facilities worldwide.

As of June 06, 2021, 177,419,783 people have been affected with the virus, with 3,838,670 of them dying (https://www.worldometers.info/coronavirus/?utm_campaign=homeAdUOA?Si as of 07-06-21). The lack of testing facilities is one of the reasons for the rising number of *COVID – 19* affected people. Due to these associated issues with RT-PCR, scientists have started work on finding alternative ways to diagnose *COVID – 19*. It has been found that due to the fast, accurate, and easily available infrastructure of radiography, X-ray and computed tomography scans can show a major contribution in the identification of *COVID – 19* (Tiwari and Jain, 2021). This has motivated the authors to do the work proposed in this manuscript. The foremost contributions to this manuscript are:

- COVID-CapsNet, COVID-RNet, COVID-3DConvNet, and COVID-DNet are the four proposed architectures for *COVID – 19* diagnosis.
- Their performance has been analyzed on relevant parameters, and it has been found that Covid-DNet has outperformed others.

The remaining portion of the manuscript is structured as follows: Findings in the area of *COVID – 19* identification through computed tomography scans are described in the Review of Literature section. The proposed methodology is explored in the methodology section. Specifics of the simulation setup and results are shown in the Simulation Environment and Experiments section. An analysis of the results is offered in the Results & Discussion section. The conclusion and future scope are offered in the last section.

REVIEW OF LITERATURE

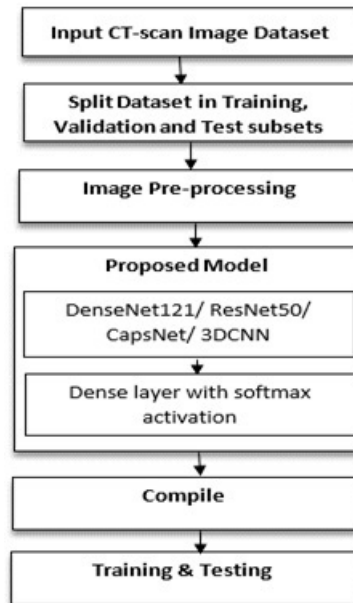
This section contains the different findings of researchers in the direction of the prediction of *COVID – 19* from chest computed tomography scans utilizing deep machine learning (Jain et al., 2019) architectures. A comparative analysis is given in table 1.

From the above review, it can be concluded that the image of chest computed tomography can play a major role in the early identification of *COVID – 19* infection in a patient. Therefore, the authors have offered a prediction system for *COVID – 19* through chest computed tomography images in this work.

Table 1. Some prominent approaches to diagnose COVID-19 from chest computed tomography scans

Author(s)	Model Detail	Dataset detail	Results
(Rahimzadeh et al., 2021)	Deep machine learning-based hybrid model designed by combination of ResNet50V2 and feature pyramid network	Collected 15589 computed tomography scans in Iran for March-April, 2020 from 95 <i>COVID – 19</i> affected patients. Also collected 48260 scans of computed tomography scan from 282 normal people	98.49% accuracy
(Zhang et al., 2020)	Deep machine learning-based 3D ResNet model	Constructed a huge database of computed tomography scans from 4154 patients. Images from 3777 patients were applied for training of model while scans of remaining patients computed tomography scan were applied for testing of model	92.49% accuracy, 94.93% sensitivity, and 91.13% specificity
(Song et al., 2021)	Proposed hybrid model by combining pre-trained ResNet50 with Feature Pyramid Network (FPN)	computed tomography scan pictures were collected in China from 88 <i>COVID – 19</i> affected patients, 100 pneumonia patients, and 86 healthy people.	93% recall, and 86% precision
(Li et al., 2020)	Deep machine learning-based 3D convolutional neural network (ConvNet)	From August 16 to February 20, 4536 chest computed tomography scans were collected from 6 hospitals in China. There were 1296 photos of <i>COVID – 19</i> affected patients, 1735 pneumonia patients, and 1325 normal persons.	90% sensitivity, 96% specificity, and 96% accuracy
(Zhao et al. 2020)	Deep convolutional neural network	There were 329 computed tomography scans in all, with 183 scans of <i>COVID – 19</i> affected patients and 146 photos of patients who were not affected with <i>COVID – 19</i> .	84.7% accuracy, 97% precision, 76.2% recall, 85.3% F1, and 82.4% area under plot Authors have developed a publically available dataset of computed tomography scans of 275 <i>COVID – 19</i> affected patients
(Zheng et al., 2020)	3D deep convolutional neural network	499 chest computed tomography scans were collected from hospitals in China from Dec-19 to Jan-20 were applied for training of the model. 131 chest computed tomography scans collected from Jan-20 to Feb-20 were applied for model testing.	90.7% sensitivity, 91.1% specificity, and 90.1% accuracy.
(Shan et al., 2020)	Deep machine learning-based VB-NET neural network.	249 <i>COVID – 19</i> affected person chest computed tomography scans were applied to train the model, and 300 <i>COVID – 19</i> affected person chest computed tomography scan photos were applied to test the model.	91.6% accuracy and faster execution time
(Wang et al., 2021)	Deep machine learning-based prediction system	A pool of 453 scans, among which 195 of <i>COVID – 19</i> and 258 of non <i>COVID – 19</i> patients	82.9% accuracy, 80.5% specificity, and 84% sensitivity

Figure 1. A proposed methodology for *COVID* – 19 identification. Four deep machine learning architectures are applied separately with computed tomography-scan image dataset.



METHODOLOGY

To develop the *COVID* – 19 identification model, four deep machine learning model architectures, including DenseNet-121, ResNet-50, Capsule Network, and 3-D ConvNet, are designed. Here, transfer learning is applied with the ResNet-50 and DenseNet-121 architectures. The steps of the methodology are depicted in Figure 1. The details of these architectures are discussed here.

Transfer Learning

An inherent benefit of the ConvNet model is that the performance of the model improves with an intensification in the quantity of training images. So, designing deep machine learning-based architectures needs a huge volume of categorized data. However, an adequate amount of data is not available in several medical-related image classification applications. The concept of transfer learning is quite effective for handling such scenarios. The idea of transfer learning is to transfer the learning gained in one domain to another domain. In the context of ConvNet, the concept of transfer learning can be applied by training parameters on one dataset and utilizing them on another dataset. In a more detailed manner, it can be stated that the first layers of a trained ConvNet model can be passed to the first layers of the second model. The other layers of the second model can be initialized randomly and trained as per the problem. After this, for the training of the network through the new dataset, either we fine-tune more layers or we allow parameters from the dense layer of the model to be adjusted. Usually, we keep the first ConvNet layer fixed as its function is edge extraction, and it is done in all problems. As we no longer train all parameters every time, the concept of transfer learning is useful in medical image-related problems that have a small labeled dataset. As shown in Figures 2 and 3, respectively, DenseNet-121 (Huang et al., 2017, Baltruschat et al., 2019, Ji et al., 2019) and Resnet-50 (Osawa et al., 2018, Wen et al., 2019) are two pre-trained deep machine learning architectures.

Figure 2. (a) DenseNet-121 model architecture. (b) Fully connected block, convolution block, and transition layer (reproduced from Osawa et al., 2018).

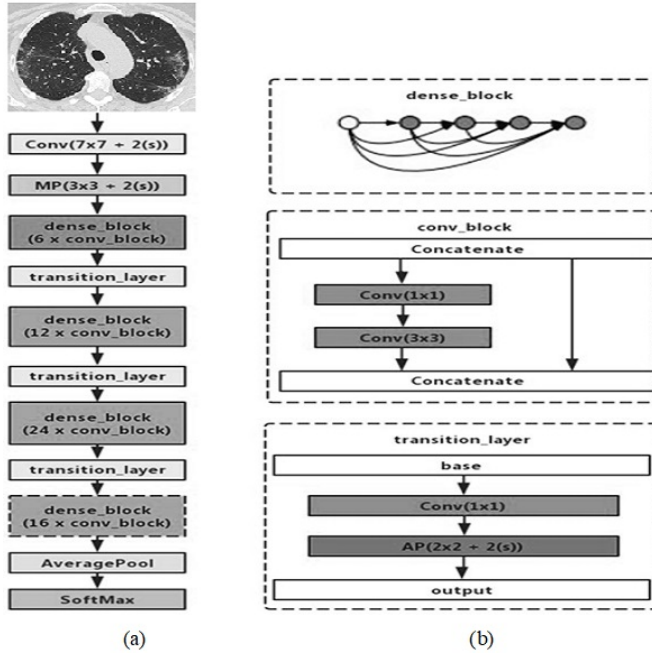
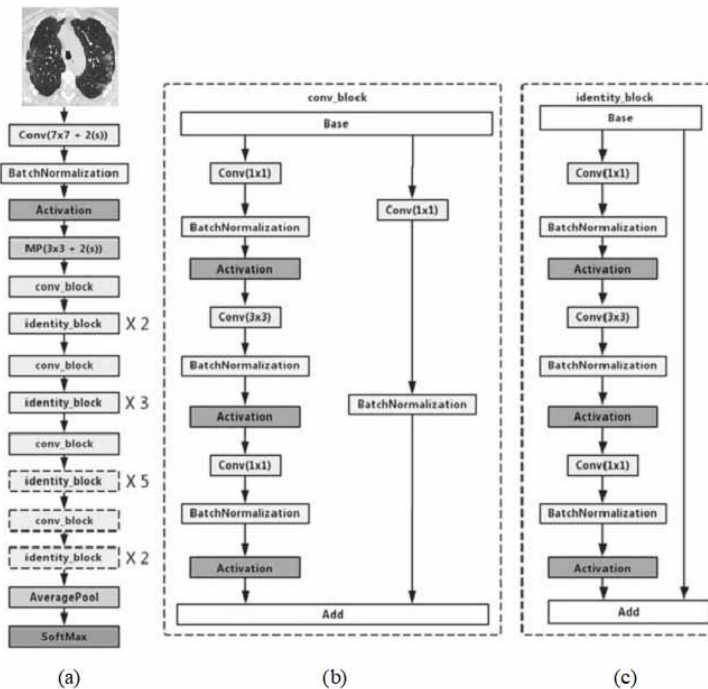


Figure 3. (a) ResNet-50 model architecture. Blocks with dotted lines denote modules that are reconfigured for transfer learning. (b) Convolution block that modifies the dimension of the input for feature mapping. (c) Identity block that does not alter the dimension of the input (reproduced from Ji et al, 2019).



Capsule Network (CapsNet)

Capsule Network, introduced in 2017 by (Sabour et al., 2017). It has offered a shift in paradigm in neural computation. In CapsNet, the traditional approach of scalar neural computation has been replaced by the vectorized approach. It arranges the neurons into clusters called capsules to efficiently learn and characterize the patterns in various object recognition applications. The capsule in CapsNet characterizes a vector to show the likelihood of the entity’s existence, and the orientation denotes the entity’s attributes (Deng et al., 2018). This squash function’s definition is as given in equation 1:

$$S_j = \frac{w_j^2}{1 + w_j^2} \frac{w_j}{w_j} \tag{1}$$

where as illustrated in equation 2, w_j is the weighted aggregate output of capsules:

$$w_j = \sum_i c_{ij} \hat{v}_{ji} \tag{2}$$

and the affine transformation defined in equation 3 is denoted by \hat{v}_{ji} :

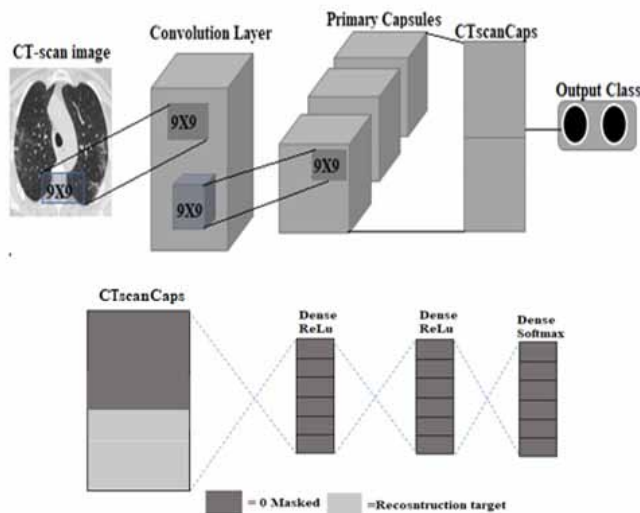
$$\hat{v}_{ji} = W_{ij} v_i \tag{3}$$

The architecture of capsules in CapsNet is shown in Figure 4.

3-D Convolution Neural Network

3D convolution calculates low-level feature representations by applying a three-dimensional filter to the dataset that moves in the x, y, and z directions (Zou et al., 2017, Alakwaa et al., 2017). The

Figure 4. CapsNet architecture for COVID – 19 diagnosis (Sabour et al. 2017)



shape of the output is identical to the cube. They are useful in the identification of events in videos and three-dimensional medical images, etc. They are not limited to three-dimensional space but can also be applied to two-dimensional space inputs. Convolution of a 3D mask is applied to perform 3D convolution. Mathematically, the response at a position on the feature-map in the layer is specified by equation 4:

$$v_{i,j}^{x,y,z} = f \left(b_{ij} + \sum_m \sum_{a=0}^{A_i-1} \sum_{b=0}^{B_i-1} \sum_{c=0}^{C_i-1} w_{ijm}^{abc} v_{(i-1)m}^{(x+a)(y+b)(z+c)} \right) \quad (4)$$

where C_i is the 3-D filter size, A_i and B_i denote the height and width of the 3D convolution filter respectively. v_{ij}^{xyz} is the response at the j^{th} feature cube of the i^{th} layer at the location (x, y, z) , w_{ijm}^{abc} denotes the specific response of the j^{th} convolution filter of the i^{th} layer at the location (a, b, c) , and the convolution filter is connected to the m^{th} feature cube of the $(i-1)^{th}$ layer. b_{ij} is biased value and $f(\bullet)$ signifies the activation function. The activation function ReLU is utilized here. It is valuable to gradient descent and backpropagation and evades the gradient disappearance problem. Figure 5 depicts the 3D ConvNet's basic design

SIMULATION ENVIRONMENT AND EXPERIMENTS

In this section, we explore the chest computed tomography image dataset and experiment with all four deep machine learning architectures as discussed in the previous section.

Dataset

A dataset of chest computed tomography scans from clinics in Sao Paulo, Brazil is taken. The total computed tomography scan is 2482, where 1252 scans are of *COVID* – 19 affected patients, while 1230 scans are of non *COVID* – 19 affected patients who have other respiratory diseases (Soares et al., 2020). Sample scans from this dataset are presented in Figure 6. It is divided into 3 subsets: train, validation, and test, with 1737, 524, and 221 scans in each subset, respectively.

Figure 5. The architecture of basic 3D ConvNet: 3-D filter is convolved to produce feature volumes with the input image in three dimensions as specified by the arrows. After downsampling utilizing pooling layers and flattening the features, a dense layer is applied for classification.

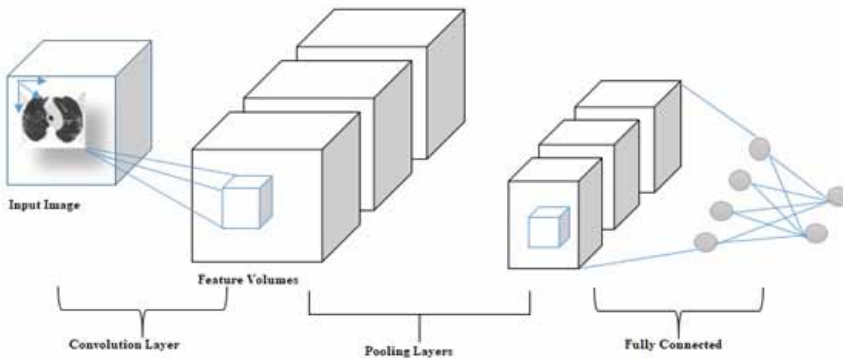
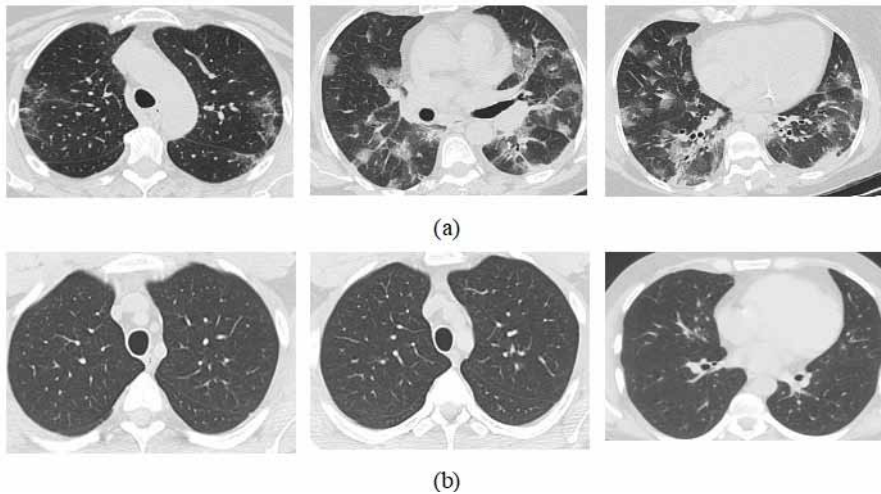


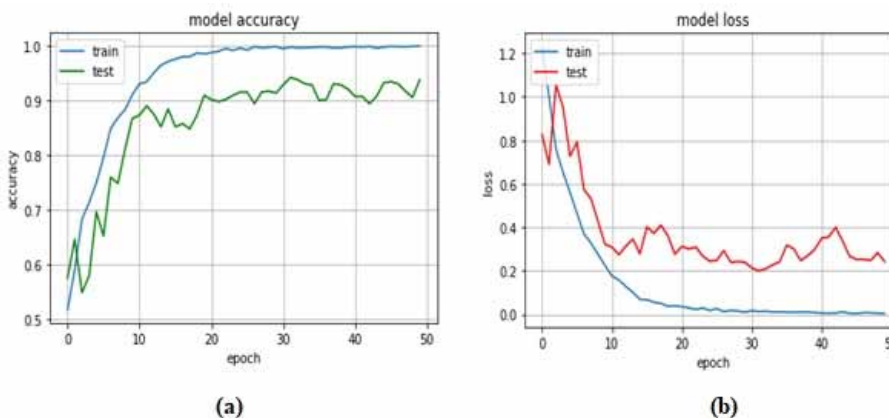
Figure 6. Sample Images for (a) computed tomography scan of patients affected by *COVID – 19* and (b) computed tomography scan of patients non-affected by *COVID – 19* , but that have other pulmonary diseases.



Experiment 1: Covid-RNet Model

In this experiment, the ResNet-50 model as discussed in the methodology section is applied and termed as Covid-RNet. The top-most layers (that is, fully connected and the classification layers) were removed. One convolution layer, two new dense layers, and a classification layer with softmax activation were applied to replace the removed layers. These newly added layers are trained utilizing features extracted from the transferred learned layers of the pre-trained ResNet-50 model. Here, transferred layers are frozen to only extract image patterns without adjusting their weights. The ResNet50 receives scans of pixel size 224*224. So, all the scans are resized to 224*224. The optimizer applied for this model is Adam. Categorical-cross entropy is applied as the loss function to calculate the loss for the Covid-RNet model. Figure 7 presents the accuracy and loss plots for the training of the Covid-RNet model. If the graph of training loss reduces to a point of stabilization, the graph of

Figure 7. Progress of accuracy (a) and loss (b) for the Covid-RNet model's training. Accuracy and Loss change sharply for the first twenty steps and stabilize after twenty steps.



learning plots reveals a satisfactory fit. The validation loss graph reaches a point of stabilization, with a narrow opening between it and the training loss. Results are provided in Table 2.

Experiment 2: Covid-CapsNet Model

As noted in the methodology section, the CapsNet model architecture is applied for COVID – 19 identification, termed as Covid-CapsNet. The model is assembled with the Adam optimizer and categorical cross-entropy as a loss function. The initial learning rate is .0012 and a total of 25 iterations with a batch size of 64 is applied. Figure 8 presents the accuracy and loss plots for the training of the Covid-CapsNet model. All the computed tomography-scans are resized to 64*64 to train and test the model. Results are offered in Table 2.

Experiment 3: Covid-DNet Model

In this experiment, the DenseNet-121 model is applied and termed as Covid-DNet. The top-most layers (that is, fully connected and the classification layers) are removed. One convolution layer, two new dense layers, and a classification layer with softmax activation are applied to replace the removed layers. These newly added layers are trained utilizing features extracted from the transferred learned layers of the pre-trained DenseNet-121 model. Here, transferred layers are frozen to only extract image patterns without adjusting their weights. All scans are resized to the size of 224*224. The optimizer applied for this model is Adam. The initial learning rate is.0015 and 50 iterations with a

Figure 8. Progress of accuracy (a) and loss (b) for the Covid-CapsNet model's training. Accuracy and Loss change sharply for the first twenty steps and stabilize after twenty steps.

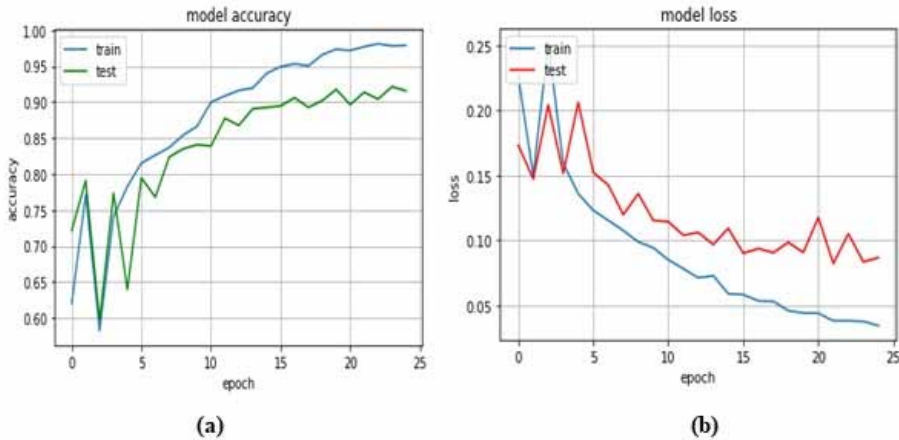


Table 2. Results of Covid-RNet and Covid-CapsNet architectures

Class/Parameter	Covid-RNet Model			Covid-CapsNet Model		
	P	S	F	P	S	F
Patients infected by COVID-19	0.99	0.98	0.98	0.89	0.99	0.94
Patients with other pulmonary diseases	0.98	0.99	0.98	0.99	0.88	0.93
Average (Macro)	0.98	0.98	0.98	0.94	0.94	0.94
Average (Weighted)	0.98	0.98	0.98	0.94	0.94	0.94
Accuracy	0.98			0.94		

batch size of 64 are applied. Figure 9 displays the accuracy and loss plots of the Covid-DNet model. Results are offered in Table 3.

Experiment 4: Covid-3DConvNet Model

In this experiment, the 3D ConvNet model is designed for *COVID – 19* identification, termed Covid-3DConvNet. The 3D-ConvNet model has 4 convolutional layers, with 2 max-pooling layers followed by 4 dense layers. A 2*2*2 max-pooling is applied to the output of the second and fourth convolutional layers. The first three dense layers consist of 2048, 512, and 512 nodes in that order. The output of the last dense layer with 2 nodes is fed to a softmax layer for classification output. Rectified Linear Input (ReLu) is applied as the activation function for the convolution output. Dropout with a rate of 0.4 is performed after the first three dense layers. Dropout is a technique applied to prevent a model from overfitting. A learning rate parameter of 0.00015 is applied. The values of β_1 , β_2 , and epsilon are 0.9, 0.999, and 0.1 respectively. The 3D-ConvNet model is trained for 100 iterations with a batch size of 32. For training and testing with the Covid-3DConvNet model, all the scans of size 128*128 are resized to 32*32*16 for training and testing. The training and validation accuracy and loss plots are plotted in Figure 10. The performance metrics are offered in Table 3.

Figure 9. Progress of accuracy (a) and loss (b) for the Covid-DNet model's training. Accuracy and Loss change sharply for the first twenty steps and stabilize after twenty steps.

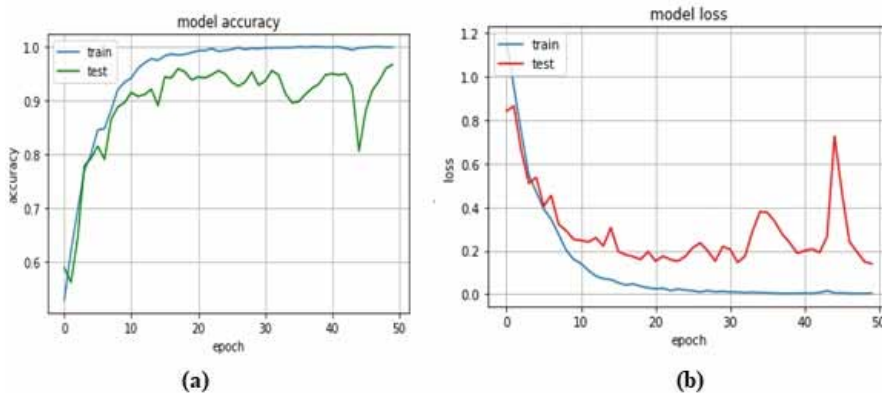
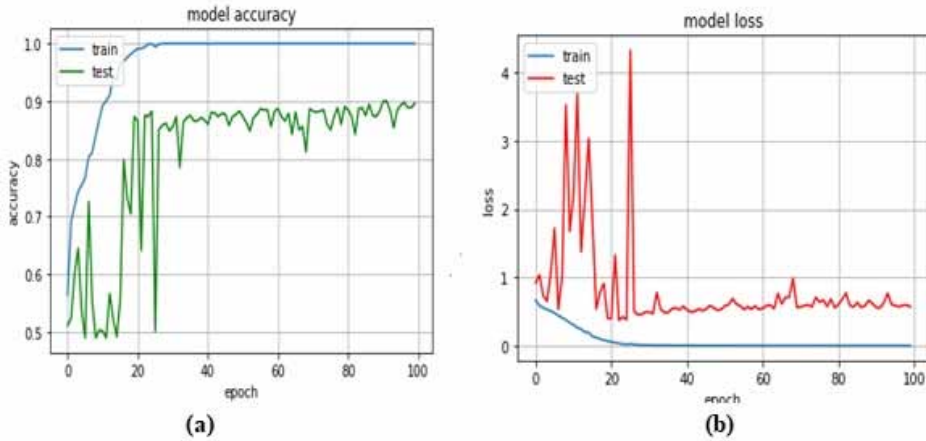


Table 3. Performance for *COVID – 19* identification utilizing Covid-DNet and Covid-3DConvNet architectures

Class/Parameter	Covid-DNet Model			Covid-3DConvNet Model		
	P	S	F	P	S	F
Patients infected by COVID-19	0.99	0.99	0.99	0.95	0.98	0.97
Patients with other pulmonary diseases	0.99	0.99	0.99	0.98	0.95	0.97
Average (Macro)	0.99	0.99	0.99	0.97	0.97	0.97
Average (Micro)	0.99	0.99	0.99	0.97	0.97	0.97
Average (Weighted)	0.99	0.99	0.99	0.97	0.97	0.97
Accuracy	0.99			0.97		

Figure 10. Progress of accuracy (a) and loss (b) for the Covid-3DConvNet model's training. Accuracy and Loss change sharply for the first twenty steps and stabilize after twenty steps.



RESULTS AND DISCUSSION

To evaluate the performance of architectures, metrics like accuracy (A), precision (P), sensitivity, and F-score (F) are applied. Accuracy is measured as the proportion of correctly classified cases. When the classes are extremely imbalanced, the precision score is a good indicator of prediction success. It denotes the proportion of genuine positives to the total number of true and false positives. The number of positive class correct predictions out of all the positive examples in the computed tomography-scan image dataset is measured by the recall. An F-Measure offers a single value that accounts for both recall and precision measures in a one value. Table 2 and Table 3 show the findings in terms of the aforementioned performance measures. It can be concluded from these tables that all of the deep machine learning architectures provide effective accuracies. The Covid-RNet, Covid-CapsNet, Covid-DNet, and Covid-3DConvNet architectures provide 0.98, 0.94, 0.99, and 0.97 accuracies, respectively.

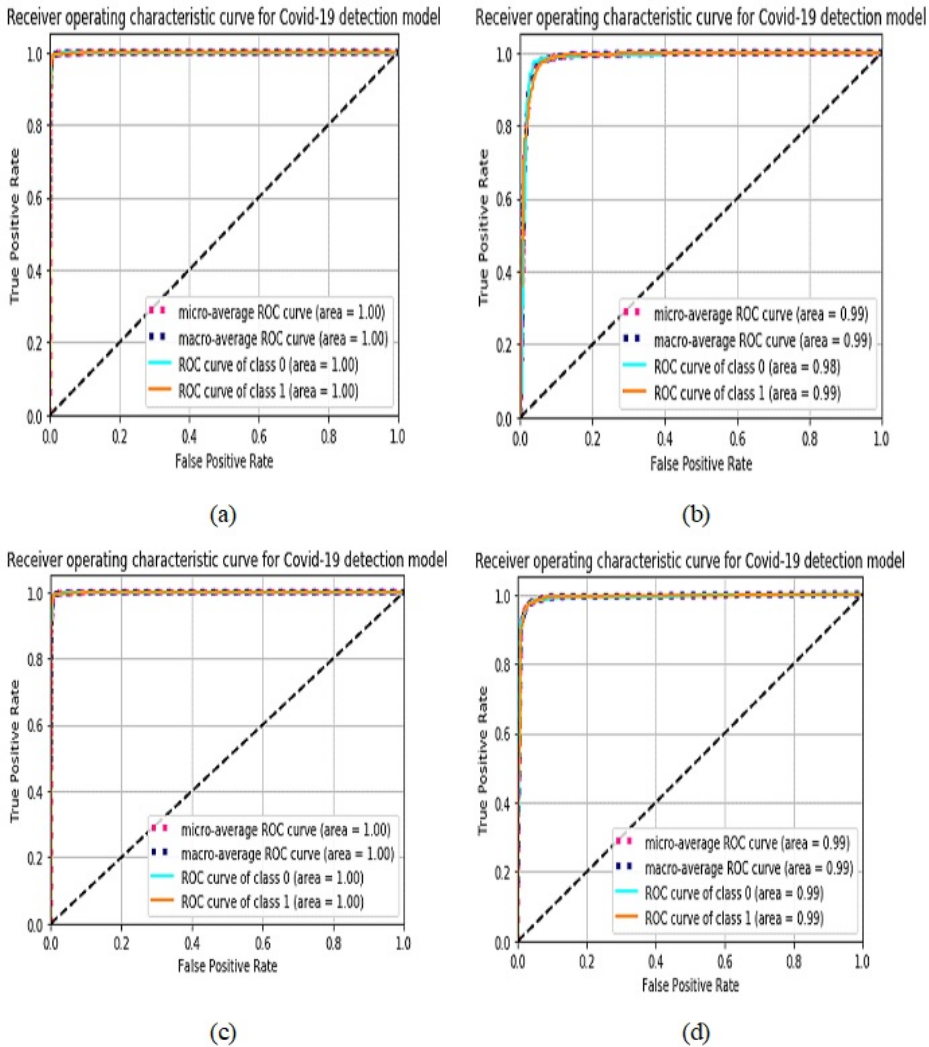
The graphs like Receiver-operating characteristic (ROC) and Area Under the Curve (AUC) are applied for more accurate analysis of the projected architectures. These plots show the ability of the classifier to differentiate different classes (Tiwari, 2020; Tiwari and Jain, 2022). Results shown in Figure 11 show the superiority of the Covid-RNet and Covid-DNet architectures over the Covid-CapsNet and Covid-3DConvNet architectures.

The performance measures are compared in Figure 12. The precision, sensitivity, F-score, and average accuracy are all 0.99 for the Covid-DNet model, which is the highest among all the Covid identification architectures. It confirms that the Covid-DNet model, which utilizes the DensNet-121 model as a pre-trained model as transfer learning, is the best among all the architectures.

CONCLUSION AND FUTURE SCOPE

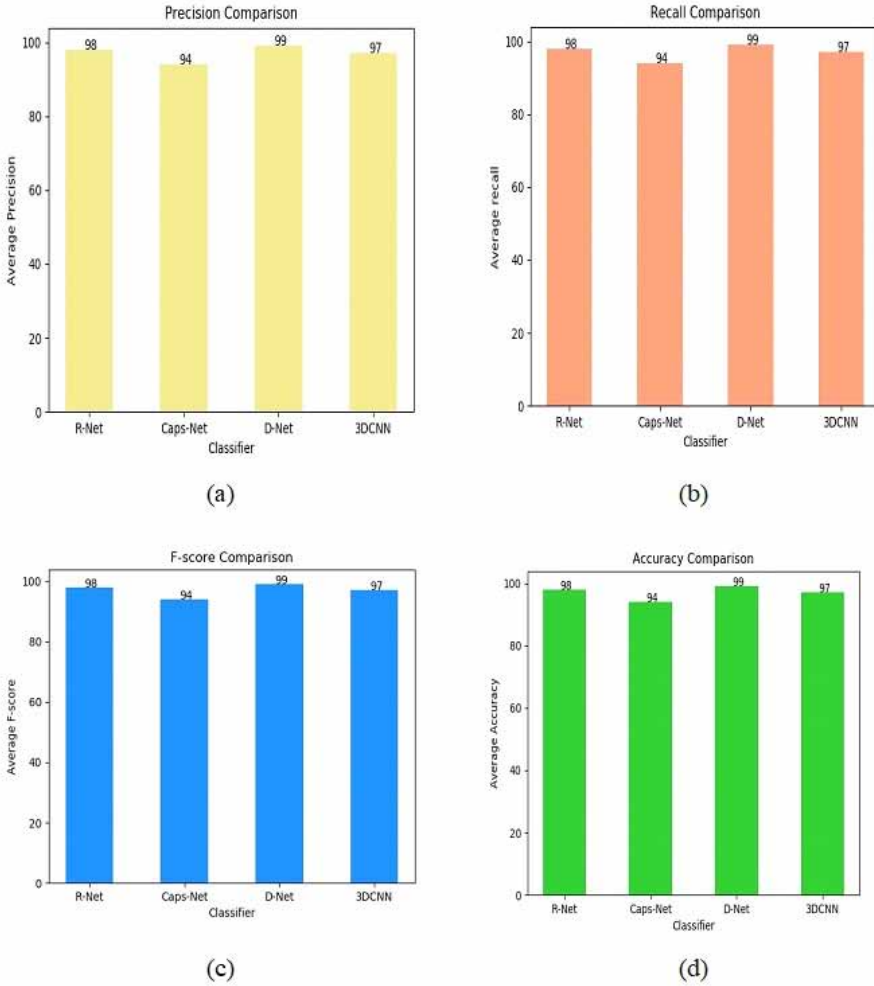
As of June 6, 2021, globally, 177,419,783 humans have been affected by the *COVID* – 19 virus and 3,838,670 have lost their lives. This has happened due to fewer testing facilities. To address this issue with current resources, the authors have designed a system that uses chest computed

Figure 11. Receiver operating characteristic plots separately for each classification model demonstrating AUC for *COVID – 19*, and normal classes (a) ROC/AUC plot for Covid-RNet Classification model, (b) ROC/AUC plot for Covid-CapsNet model, (c) ROC/AUC plot for Covid-DNet Classification model, (d) ROC/AUC plot for Covid-3DConvNet Classification model



tomography-scan pictures to diagnose *COVID – 19* infection. Four deep machine learning-based architectures have been designed utilizing DNet, RNet, CapsNet, and 3D ConvNet. Architectures are trained and tested on an online chest computed tomography-scan image dataset. Their performance is matched on the scale of accuracy, precision, sensitivity, F-score, and AUC. It is found that the model designed utilizing DNet had the highest accuracy of 99%. This model is one step in the direction of diagnosing *COVID – 19* affected patients by utilizing an easily available radiography structure. Moreover, it will give a prompt result at a very cheap rate. This can help healthcare workers in their fight against this pandemic. Therefore, it can be concluded that the chest computed tomography scan diagnosis utilizing deep machine learning architectures

Figure 12. Comparative analysis of (a) precision, (b) sensitivity, (c) F-score (d) accuracy for Covid-RNet, CapsNet, DNet, and 3D ConvNet architectures



is sensitive to *COVID – 19* identification. As a future scope, the authors have planned to combine chest computed tomography scan results with some other clinical tests to get a more accurate prediction of *COVID – 19* .

FUNDING AGENCY

Publisher has waived the Open Access publishing fee.

REFERENCES

- Alakwaa, W., Nassef, M., & Badr, A. (2017). Lung cancer detection and classification with 3D convolutional neural network (3D-CNN). *Lung Cancer (Amsterdam, Netherlands)*, 8(8), 1–10.
- Alpaydin, A. O., Gezer, N. S., Simsek, G. O., Tertemiz, K. C., Kutsoylu, O. O., Zeka, A. N., Guzel, I., Soyuturk, M., Sayiner, A. A., & Oguz, V. A. (2021). Clinical and radiological diagnosis of non-SARS-CoV-2 viruses in the era of COVID-19 pandemic. *Journal of Medical Virology*, 93(2), 1119–1125. doi:10.1002/jmv.26410 PMID:32770738
- Angelov, P., & Almeida Soares, E. (2020). SARS-CoV-2 CT-scan dataset: A large dataset of real patients CT scans for SARS-CoV-2 identification. *MedRxiv*, 1–8.
- Baltruschat, I. M., Nickisch, H., Grass, M., Knopp, T., & Saalbach, A. (2019). Comparison of deep learning approaches for multi-label chest X-ray classification. *Scientific Reports*, 9(1), 1–10.
- Bhardwaj, R., & Agrawal, A. (2020). Likelihood of survival of coronavirus in a respiratory droplet deposited on a solid surface. *Physics of Fluids*, 32(6), 1–7.
- Deng, F., Pu, S., Chen, X., Shi, Y., Yuan, T., & Pu, S. (2018). Hyperspectral image classification with capsule network using limited training samples. *Sensors (Basel)*, 18(9), 1–22.
- Huang, G., Liu, Z., Van Der Maaten, L., & Weinberger, K. Q. (2017). Densely connected convolutional networks. In *Proceedings of the IEEE conference on computer vision and pattern recognition* (pp. 4700–4708). IEEE.
- Jahangir, M. A., Muheem, A., & Rizvi, M. F. (2020). Coronavirus (COVID-19): History, current knowledge and pipeline medications. *Int J Pharm Pharmacol*, 4(1), 1–9.
- Jain, A., Tiwari, S., & Sapra, V. (2019). Two-phase heart disease diagnosis system using deep learning. *International Journal of Control and Automation*, 12(5), 558–573.
- Jain, A., Yadav, K., Alharbi, H. F., & Tiwari, S. (2022). IOT & AI enabled three-phase secure and non-invasive covid 19 diagnosis system. *Computers. Materials and Continua*, 71(1), 423–438.
- Lee, C. Y. P., Lin, R. T., Renia, L., & Ng, L. F. (2020). Serological approaches for COVID-19: Epidemiologic perspective on surveillance and control. *Frontiers in Immunology*, 11, 1–7.
- Li, L., Qin, L., Xu, Z., Yin, Y., Wang, X., Kong, B., & Xia, J. et al. (2020). Artificial intelligence distinguishes COVID-19 from community acquired pneumonia on chest CT. *Radiology*, 1–16.
- Osawa, K., Tsuji, Y., Ueno, Y., Naruse, A., Yokota, R., & Matsuoka, S. (2018). *Second-order optimization method for large mini-batch: Training resnet-50 on imagenet in 35 epochs*. arXiv preprint arXiv:1811.12019.
- Rahimzadeh, M., Attar, A., & Sakhaei, S. M. (2021). A fully automated deep learning-based network for detecting covid-19 from a new and large lung ct scan dataset. *Biomedical Signal Processing and Control*, 68, 1–14.
- Sabour, S., Frosst, N., & Hinton, G. E. (2017). *Dynamic routing between capsules*. arXiv preprint arXiv:1710.09829.
- Shan, F., Gao, Y., Wang, J., Shi, W., Shi, N., Han, M., . . . Shi, Y. (2020). *Lung infection quantification of COVID-19 in CT images with deep learning*. arXiv preprint arXiv:2003.04655.
- Song, Y., Zheng, S., Li, L., Zhang, X., Zhang, X., Huang, Z., & Yang, Y. et al. (2021). Deep learning enables accurate diagnosis of novel coronavirus (COVID-19) with CT images. *IEEE/ACM Transactions on Computational Biology and Bioinformatics*, 14(8), 1–8.
- Tahamtan, A., & Ardebili, A. (2020). Real-time RT-PCR in COVID-19 detection: Issues affecting the results. *Expert Review of Molecular Diagnostics*, 20(5), 453–454.
- Tiwari, S. (2020). A comparative study of deep learning models with handcraft features and non-handcraft features for automatic plant species identification. *International Journal of Agricultural and Environmental Information Systems*, 11(2), 44–57.
- Tiwari, S., & Jain, A. (2021). Convolutional capsule network for COVID-19 detection using radiography images. *International Journal of Imaging Systems and Technology*, 31(2), 525–539.

- Tiwari, S., & Jain, A. (2022). Lightweight capsule network architecture for detection of COVID-19 from lung CT scans. *International Journal of Imaging Systems and Technology*, 32(2), 419–434.
- Wang, S., Kang, B., Ma, J., Zeng, X., Xiao, M., Guo, J., & Xu, B. et al. (2021). A deep learning algorithm using CT images to screen for Corona Virus Disease (COVID-19). *European Radiology*, 31, 6096–6104.
- Wen, L., Li, X., & Gao, L. (2020). A transfer convolutional neural network for fault diagnosis based on ResNet-50. *Neural Computing & Applications*, 32(10), 1–14.
- Worldometers.info. (n.d.). https://www.worldometers.info/coronavirus/?utm_campaign=homeAdUOA?Si
- Zhang, K., Liu, X., Shen, J., Li, Z., Sang, Y., Wu, X., & Wang, G. et al. (2020). Clinically applicable AI system for accurate diagnosis, quantitative measurements, and prognosis of COVID-19 pneumonia using computed tomography. *Cell*, 181(6), 1423–1433.
- Zhao, J., Zhang, Y., He, X., & Xie, P. (2020). *Covid-ct-dataset: a ct scan dataset about covid-19*. arXiv preprint arXiv:2003.13865.
- Zheng, C., Deng, X., Fu, Q., Zhou, Q., Feng, J., Ma, H., ... Wang, X. (2020). Deep learning-based detection for COVID-19 from chest CT using weak label. *MedRxiv*, 1-13.
- Zou, L., Zheng, J., Miao, C., Mckeown, M. J., & Wang, Z. J. (2017). *3D CNN based automatic diagnosis of attention deficit hyperactivity disorder using functional and structural MRI*. Academic Press.

Shamik Tiwari is currently working as Sr. Associate Professor in Department of Virtualization at SoCS, University of Petroleum and Energy Studies, Dehradun. His are of interest are digital image processing, computer vision, bio-metrics, cloud computing and health informatics. He has written many national and International publications including books in these fields.

Anurag Jain is currently serving at the University of Petroleum and Energy Studies, Dehradun as an Associate Professor in the School of Computer Science. He is in the field of academia for the last 18 years. He has published around 50 research papers in renowned journals and conferences. 14 students have successfully defended their M. Tech. thesis under his guidance. His research area is in the domain of scheduling and load balancing in cloud computing, healthcare, machine learning, and data science. Currently, he is guiding 5 Ph.D. students in their research work.

Sunil Kumar Chawla is working as an Assistant Professor in the Department of Computer Science and Engineering, Chandigarh University, Mohali, Punjab, India. He is currently pursuing his doctorate from IKG Punjab Technical University. He is having teaching experience of more than 15 years. His research interests lie in Digital Image Processing, Biometrics, Image Segmentation, and Machine Learning. He is a member of IEEE and other professional societies like ISTE, CSTA, IAENG, and IETE. He has more than 30 Publications in International journals of repute indexed in Scopus, ESCI, Google Scholar and other eminent databases. He has been associated with many reputed international conferences in the capacity of Technical Programme Committee member. He is serving as a reviewer of several reputed journals. He has published a book entitled Segmentation and Normalization of Iris for Human Recognition with Lambert Academic Publishing, Germany. He has filed two patents. He is Guest Editor of two books under CRC Press, Taylor and Francis, USA and many special issues of reputed international journals.